Iminopropadienones RN=C=C=C=O and bisiminopropadienes RN=C=C=C=NR: Matrix infrared spectra and anharmonic frequency calculations.

Didier Bégué, Isabelle Baraille, Heidi Gade Andersen, Curt. Wentrup

Iminopropadienones RN=C=C=C=O and bisiminopropadienes RN=C=C=C=NR: Matrix infrared spectra and anharmonic frequency calculations

Didier Bégué, Isabelle Baraille, Heidi Gade Andersen, and Curt Wentrup

Citation: The Journal of Chemical Physics **139**, 164314 (2013); doi: 10.1063/1.4826647
View online: http://dx.doi.org/10.1063/1.4826647
View Table of Contents: http://scitation.aip.org/content/aip/journal/jcp/139/16?ver=pdfcov
Published by the AIP Publishing

Iminopropadienones RN=C=C=C=O and bisiminopropadienes RN=C=C=C=NR: Matrix infrared spectra and anharmonic frequency calculations

Didier Bégué,[1,a)] Isabelle Baraille,[1] Heidi Gade Andersen,[2] and Curt Wentrup[2,a)]
[1]*Institut des Sciences Analytiques et de Physico-Chimie pour l'Environnement et les Matériaux, Equipe Chimie Physique, UMR 5254, Université de Pau et des Pays de l'Adour, 64000 Pau, France*
[2]*School of Chemistry and Molecular Biosciences, The University of Queensland, Brisbane, Queensland 4072, Australia*

(Received 8 July 2013; accepted 8 October 2013; published online 29 October 2013)

Methyliminopropadienone MeN=C=C=C=O **1a** was generated by flash vacuum thermolysis from four different precursors and isolated in solid argon. The matrix-isolation infrared spectrum is dominated by unusually strong anharmonic effects resulting in complex fine structure of the absorptions due to the NCCCO moiety in the 2200 cm^{-1} region. Doubling and tripling of the corresponding absorption bands are observed for phenyliminopropadienone PhN=C=C=C=O **1b** and bis(phenylimino)propadiene PhN=C=C=C=NPh **9**, respectively. Anharmonic vibrational frequency calculations allow the identification of a number of overtones and combination bands as the cause of the splittings for each molecule. This method constitutes an important tool for the characterization of reactive intermediates and unusual molecules by matrix-isolation infrared spectroscopy.
 [http://dx.doi.org/10.1063/1.4826647]

INTRODUCTION

Matrix-isolation infrared spectroscopy is an invaluable method for the characterization of reactive intermediates and unusual molecules.[1] Moreover, the development of accurate quantum mechanical methods for the calculation of fundamental vibrational frequencies has made combined experimental-computational studies almost mandatory in the investigation of such compounds. However, in many cases, a full characterization of experimental spectra requires calculation of overtones and combination bands, which cannot be carried out with the commonly available computational programs. For this purpose, a variational method to perform frequency calculations in the mechanical and electrical anharmanonic approximations has been developed.[2–4] We have used this method recently in an analysis of the matrix-isolation IR spectra of nitrile imines R–C≡N^+–N^-–R′.[5] Here, we have applied the method to another experimental problem, viz., the interpretation of the infrared spectra of iminopropadienones RN=C=C=C=O and bisiminopropadienes, RN=C=C=C=NR, which feature unusually complex fine structure.

Iminopropadienones, RN=C=C=C=O, have been generated by flash vacuum thermolysis (FVT) of several different precursors, the most typical being 5-methylene derivatives **2** of Meldrum's acid and isoxazolo[5,4-*d*]pyrimidinones derivatives **3** (Scheme 1).[6]

While the aryliminopropadienones have been the subject of extensive chemical and spectroscopic studies,[6,7] the alkyliminopropadienones are much less well known.[8] The methyl derivative **1a** is a reactive intermediate, which can only be isolated at temperatures below −100 °C or investigated directly in the gas phase.[9,10] In particular, the infrared spectrum has not been reported and, as elaborated below, its interpretation is not straightforward.

COMPUTATIONAL METHOD

Calculations of geometries, energies, and harmonic vibrational frequencies of iminopropadienones MeNCCCO **1a**, PhNCCCO **1b**, and PhNCCCNPh **9** and some of their isotopomers were performed with the B3LYP hybrid functional[11] using the 6-31G* basis set implemented in the Gaussian 2009 program suite.[12]

Commonly available electronic structure packages can perform calculations of the fundamental vibrational harmonic frequencies routinely. The related IR intensities are calculated within the so-called double harmonic approximation, in which the vibrational wavefunction is computed as a product of the harmonic oscillator functions and the dipole moment function developed as a linear function of normal coordinates. The intensity of the sth fundamental mode is proportional to the square of the first derivative of the dipole moment with respect to the normal coordinate Q_s. However, the presence

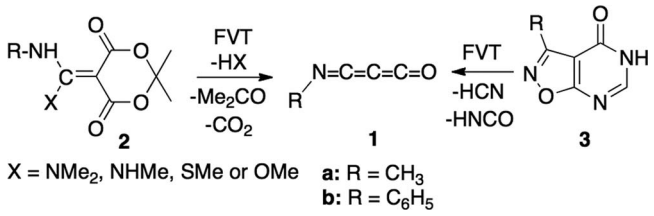

SCHEME 1. Meldrum's acid derivatives and isoxazolopyrimidinone precursors for generation of iminopropadienones R–N=C=C=C=O **1** by FVT.

a)Authors to whom correspondence should be addressed. Electronic addresses: didier.begue@univ-pau.fr and wentrup@uq.edu.au.

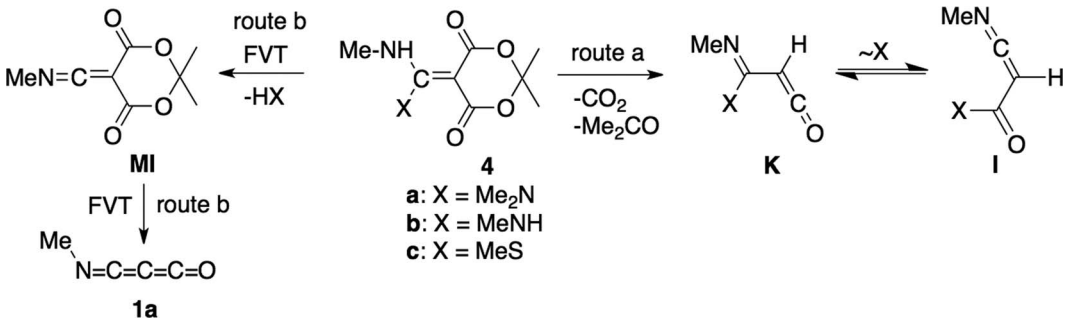

SCHEME 2. Three Meldrum's acid-based precursors of MeNCCCO **1a**.

of overtones and combination bands in the infrared spectra is a manifestation of the breakdown of the double-harmonic approximation. The calculation of their intensities is mandatory in order to determine which of these non-fundamental transitions are active and to assign all the experimental bands. Since both mechanical (anharmonicity of the potential) and electrical (nonlinear dependence of the dipole moment on the normal coordinates) anharmonicities are expected to give intensity to non-fundamental transitions, these two effects have to be considered in the treatment of transition energies and related vibrational wavefunctions. The frequency calculations in the mechanical anharmonic approximation were carried out using a variational method a developed by Bégué *et al.*[2] Using this method, implemented in the P_Anhar.v2.0 program,[3] it was possible to compute all the vibrational frequencies (fundamental, combination bands, and overtones) that contribute to the mid- and near-infrared spectrum of the cumulenes studied in this paper. In addition, the activity of each mode was also calculated in the electrical anharmonic approximation using a capability included in the latest version of the program following the method developed by Baraille *et al.*[4]

RESULTS AND DISCUSSION

Me-N=C=C=C=O 1a

Methyliminopropadienone **1a** was generated by FVT of four different precursors with matrix isolation of the products in solid Ar at ∼10 K. The first three precursors were the Meldrum's acid derivatives **4a–4c** (Scheme 2), which on FVT generate the thermally interconverting ketene K and the ketenimine I (route a), both of which have been identified by IR and mass spectrometry.[8,13] Route a operates at lower temperatures; hence an appreciable amount of ketenimine I is observed in the matrix IR spectrum resulting from FVT at 600 °C (Figure S1 in the supplementary material[21]). A very small amount still persists in the product from FVT at 800 °C (peak I, Figure 1, 2076 cm^{-1}). The second route, route b (Scheme 2) becomes dominant at higher FVT temperatures and proceeds via the transient ketenimine MI to produce rather pure matrixes of the iminopropadienone. This way the three precursors **4a–4c** all afford MeNCCCO **1a** together with the necessary byproducts CO_2, acetone and dimethylamine, methylamine, or methanethiol. The amidine drivative

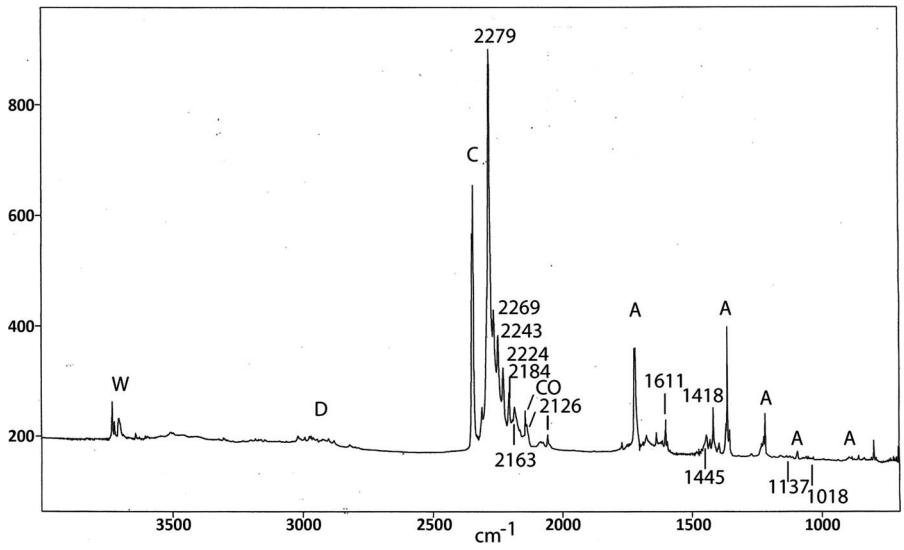

FIG. 1. IR spectrum of MeN=C=C=C=O **1a** formed by FVT of 5-[(dimethylamino)(methylamino)methylene]-Meldrum's acid **4a** at 800 °C and isolated in Ar matrix at 14 K. W: water; C: carbon dioxide (2345 and 2340 cm^{-1}); CO: carbon monoxide (2138 cm^{-1}); A: acetone (1721, 1361, 1216, 1094, and 883 cm^{-1}); D: dimethylamine (3193, 2973, 2838, 2793, 2789, 1482, 1478, and 1457 cm^{-1}); I: ketenimine intermediate I (Scheme 2) (2076 cm^{-1}). Bands assigned to $MeNC_3O$ **1a**: 2279 (vs)(ν_{as} NCCCO), 2269, 2243, 2224, 2214 (shoulder), 2184, 2163 (ν_s NCCCO), 2126, 1611, and 1418 cm^{-1} together with very weak bands at 1445, 1433, 1137, 1018, and 558 cm^{-1}.

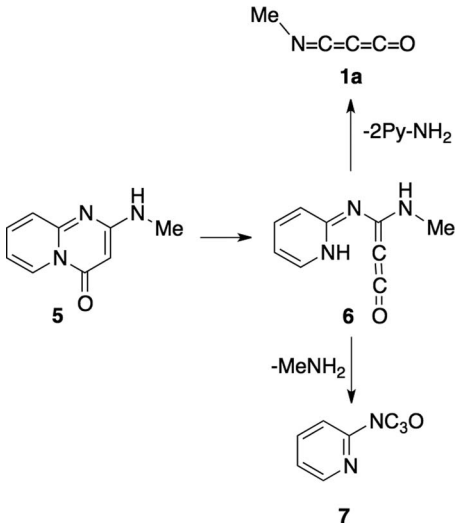

SCHEME 3. The pyridopyrimidinone precursor **5** yielding MeNCCCO **1a** and 2-PyNCCCO **7**.

4a is the best precursor; hence most experiments were performed with this compound. Iminopropadienone **1a** is highly unstable, and investigation of the IR spectrum requires matrix isolation at cryogenic temperatures (Figure 1).

A fourth precursor, the pyrido[1,2-*a*]pyrimidinone **5**, undergoes more complicated thermolysis, yielding a mixture of MeNCCCO **1a** and 2-pyridyliminopropadienone **7** (∼1:1) in the temperature range 700–900 °C (Scheme 3). This reaction takes place via the intermediate ketene **6** with 2-aminopyridine and methylamine as by-products. The formation of aryliminopropadienones by this method has been elucidated.[14] The FVT of **5** is important because the same structured IR absorption band of **1a** in the 21 000–2300 cm^{-1} is obtained as seen in Figure S2 (supplementary material).[21] The IR spectrum of 2-pyridyliminopropadienone **7** has been described previously and is dominated by a very strong absorption due to the antisymmetric cumulenic stretch at 2249 cm^{-1} and a weak symmetric stretch at 2128 cm^{-1}.[14,15]

Previous calculations[7] on the parent compound, HNCCCO, at the HF level indicated the existence of a nearly linear form, in the following referred to as "linear," as well as a "bent" form, but only the "linear" form of **1a** was located at the MP2 level.[9] Similarly, we find only the "linear" form of **1a** at the B3LYP/6-31G* level. However, local LCCSD(T)/cc-pVTZ calculations[16] indicate that the "linear" form **1a** is the ground state, but a "bent" form **1a′** is predicted at only 0.03 kcal/mol higher energy (see Figure 2), and the barrier to linearization is ∼3 kcal/mol. The related isoelectronic molecule carbon suboxide, O=C=C=C=O, is known to be bent with a CCC angle of 156° in the gas phase, but with an extremely flat potential well and a barrier of only ∼18 cm^{-1} to linearization.[17] Thus, like O=C=C=C=O, **1a** can be described as quasi-linear.

The calculated IR spectral data for the "linear" and "bent" forms **1a** and **1a′** at the LCCSD(T)/cc-pVTZ level are sufficiently different to permit the conclusion that the linear form **1a** is being observed experimentally (Table I). In particular, the symmetric stretch of the NCCCO moiety is predicted at 2166 for the "linear" and at 2222 for the "bent" structure. The experimental value is 2163 cm^{-1} (Tables I and II). Other wavenumbers are also affected, i.e., those implying NCC moieties (α_{NCC} and ν_{NC}). The full spectroscopic description of the vibrational modes of **1a** at B3LYP/6-31G*, B3LYP/6-311++G(2df,2pd), and hybrid CCSD(T)/cc-pVDZ//B3LYP/6-31G* (see Ref. 18) levels are also presented in Table I, and the relevant data necessary for an understanding of the fine structure of the cumulene band is summarized in Table II. As is usually the case,[1] the experimental numbers are mostly a little smaller than the calculated ones. The vibrational modes discussed here are depicted in Figure 3.

The IR spectrum of Me-N=C=C=C=O **1a** in Ar matrix exhibits an unexpected and unusually complex absorption with a strong maximum at 2279 cm^{-1} (ν_{12} ; Table II, Figure 1, and Figures S1 and S2 in the supplementary material[21]). The same pattern is obtained by using the four different precursors, and the splitting cannot be removed by annealing; therefore, it is not likely to be due to different matrix sites. The pronounced structure can be ascribed to the occurrence of several active overtones and combination modes, namely $\nu_3 + \nu_{10}$ (I = 1.23 km mol^{-1}), $2\nu_6$ (I = 0.39 km mol^{-1}), and $\nu_5 + \nu_6$ (I = 0.10 km.mol^{-1}), located at 2255, 2229, and 2207 cm^{-1}, respectively (Table II). The $2\nu_6$ and $\nu_5 + \nu_6$ active bands explain the observed band structure unambiguously. Because these additional bands are associated with an angular distortion mode of the methyl group ν_6 (I = 40.3 km mol^{-1}), they are not expected for differently substituted iminopropadienones. Conversely, the $\nu_3 + \nu_{10}$ mode involves the NCCCX moiety (X = O or N) and can therefore be expected to cause limited fine structure for all iminopropadienone derivatives including the three systems studied here, **1a**, **1b**, and **9**.

A medium-strength band associated with the symmetrical NCCCO stretching is calculated at 2179 cm^{-1} (experimental value 2163 cm^{-1}). In addition, an overtone $\nu_4 + \nu_6$ – again

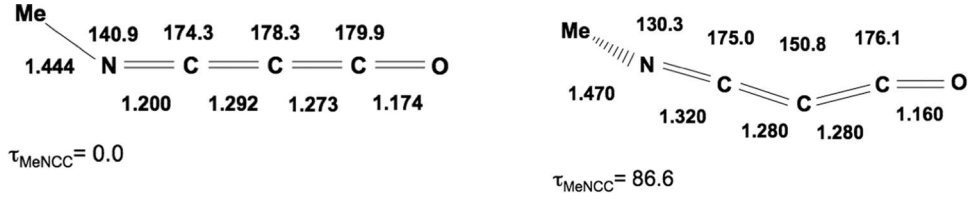

FIG. 2. Calculated "linear" and "bent" structures of Me-NCCCO (**1a** and **1a′**) at the LCCSD(T)/cc-pVTZ level (bond lengths in Å; bond angles and dihedral angles τ in degrees (°)). The energy difference between **1a** and **1a′** is ΔE = 0.03 kcal mol^{-1}. The energy barrier for linearization in **1a′** is 3.1 kcal mol^{-1}.

TABLE I. Experiental wavenumbers for methyliminopropadienone and calculated anharmonic wavenumbers for **1a** ("linear") and **1a′** ("bent").[a]

		1a					**1a′**
			Intensity (km/mol)	ν_{theor} (cm^{-1})			ν_{theor} (cm^{-1})
Mode	Description	Experimental	a	a/a′	b	c	b
1	α_{CCO}		16.2	536/532	517	520	569
2	α_{CCO}	558	23.2	553/555	550	552	583
3	α_{NCC}		6.2	636/634	642	652	724
4	ν_{NC}	1018	10.7	1024/1031	1033	1030	1069
5	ω_{CH}		0.0	1088/1085	1093	1068	1125
6	δ_{CH3}	1137	40.3	1116/1127	1127	1116	1167
7	$\delta_{CH3\ umbrella}$	1418	116.4	1432/1409	1427	1404	1455
8	σ_{CH3}	1433	7.8	1447/1443	1444	1426	
9	τ_{CH3}	1445	7.2	1464/1456	1490	1454	
10	ν_{NCCCO}	1611	175.2	1627/1634	1609	1603	1614
11	$\nu_{CC\ sym,\ NCCCO}$	2163	0.1	2180/2184	2166	2161	2222
12	$\nu_{CC,\ asym,\ NCCCO}$	2279	>500	2279/2285	2285	2281	2288

[a]a : B3LYP/6-31G*; a′ : B3LYP/6-311++G(2df,2pd); b : LCCSD(T)/cc-pVTZ; c: hybrid CCSD(T)/cc-pVDZ//B3LYP/6-31G*.

TABLE II. Anharmonic wavenumbers ν (cm^{-1}), principal assignments, and dominant contribution (%) for Me-NCCCO **1a** in the range 2100–2300 cm^{-1}.

Me-NCCCO **1a**				
			Wavenumbers (cm^{-1})	
Mode	Description	%	ν_{exp}	ν_{theor}
$\nu_4+\nu_6$	$\alpha_{CCO} + \delta_{CH3}$	79	2126	2136
ν_{11}	$\nu_{CC\ sym,\ NCCCO}$	92	2163	2179
$\nu_5+\nu_6$	$\omega_{CH} + \delta_{CH3}$	85	2184	2207
$2\ \nu_6$	δ_{CH3}	89	2224	2229
$\nu_3+\nu_{10}$	$\alpha_{NCC} + \nu_{NCCCO}$	94	2243	2255
ν_{12}	$\nu_{CC,\ asym,\ NCCCO}$	95	2279	2279

involving the angular distortion of the methyl group (I = 1.21 km mol^{-1}) – is predicted at 2136 cm^{-1}. The weak experimental peak is found at 2126 cm^{-1} (Figure 1 and Table II).

In summary, the infrared spectrum of **1a** is well accounted for by the anharmonic vibrational calculations.

Ph-N=C=C=C=O 1b

1b was generated by FVT of **2b** (X = NMe_2) at 600 °C and isolated in solid Ar at 15 K. The matrix IR spectrum is shown in Figure S3 (supplementary material).[21] The principal features are the doublet at 2247/2243 cm^{-1} assigned to the

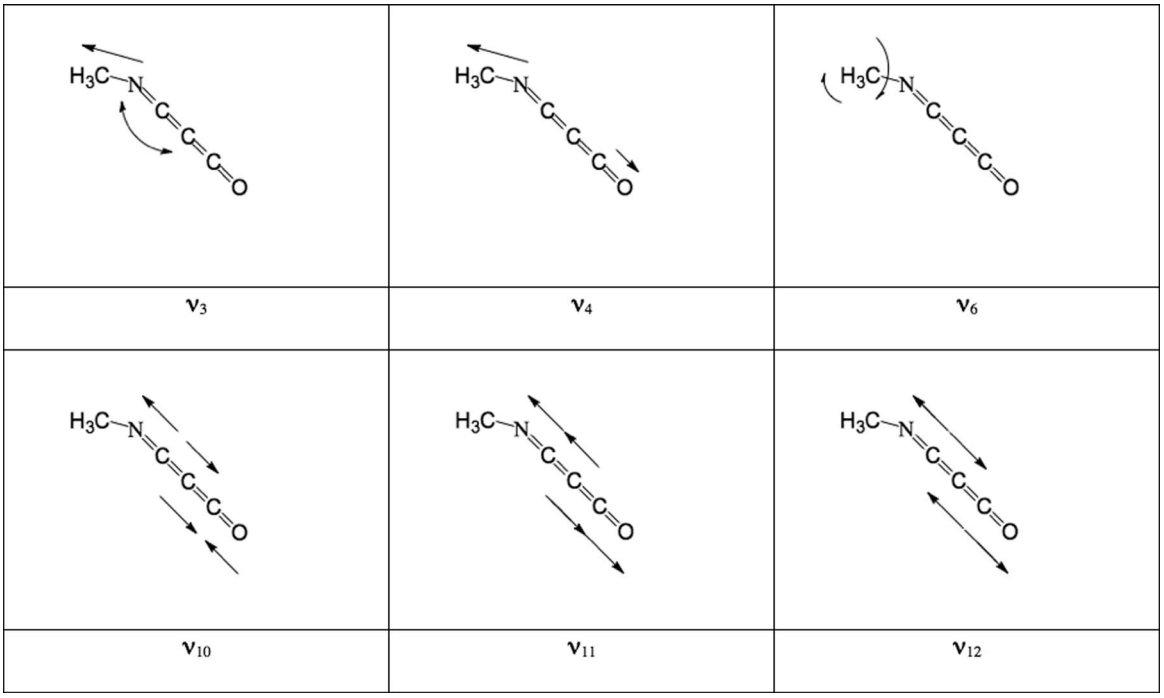

FIG. 3. Description of the modes involved in active fundamental overtones and combination bands in the 2100–2300 cm^{-1} region for **1a**.

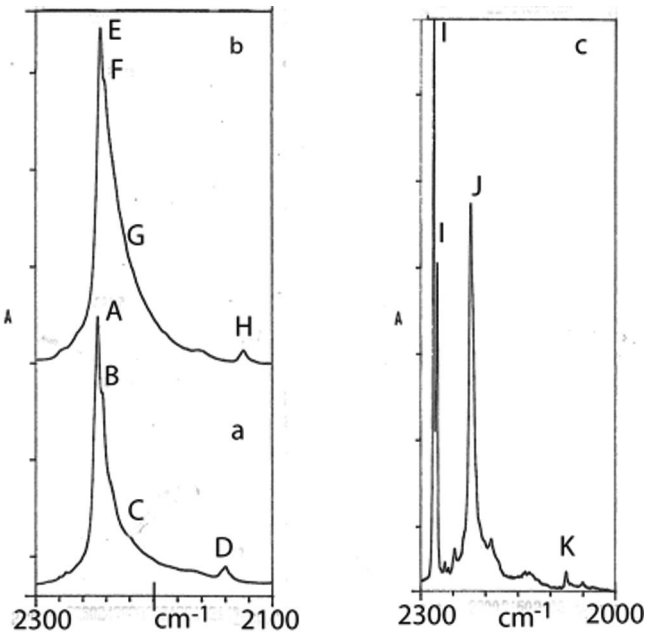

FIG. 4. IR spectra (Ar matrix, 15 K) of (a) PhNCCCO **1b**, (b) Ph^{15}NCCCO, and (c) PhNCC^{13}CO in the cumulene region. The compounds were generated by FVT of **2b** at 600 °C (cf. Figure S3). Peaks A: 2247; B: 2243; C: 2220; D: 2140; E: 2245; F: 2242; G: ∼2220; H: 2124; I: $^{13}CO_2$; J: 2222; K: 2080 cm^{-1}.

antisymmetic stretching absorption, and a weak symmetrical stretch near 2140 cm^{-1} (peaks A, B, and D, Figure 4(a)). The calculated vibrational modes for **1b** and its ^{15}N and ^{13}C isotopomers at the B3LYP/6-31G* level are presented in full in Table S2 in the supplementary material[21] and in part in Table III. The relevant vibrational modes are depicted in Figure 5.

The major absorption at 2247/2243 cm^{-1} (peaks A and B, Figure 4(a)) is a doublet with the weaker component at 2243 cm^{-1} assigned to the fundamental antisymmetric stretching vibration ν_{25} and the stronger component at 2247 cm^{-1} assigned to the combination mode $\nu_{12} + \nu_{17}$ (Table III and peaks B and A in Figure 4(a)). Again, the splitting of this absorption cannot be removed by annealing and thus cannot be ascribed to site splitting. Indeed, the evaluation of the $\nu_{12} + \nu_{17}$ vibrational wavefunction obtained from the diagonalization of the Shrödinger vibrational Hamiltonian shows that the $\nu_{12} + \nu_{17}$ combination band borrows intensity from the intense fundamental mode ν_{25} for reasons of both energetic closeness and strong anharmonic coupling through the cubic constants which describe the potential energy surface.[19] As the two modes ν_{12} and ν_{17} correspond to the δ_{CH} and $\nu_{CC,cycle}$ modes of the phenyl group, respectively, there is no significant displacement of this mode for the ^{15}N isotopomer (Table III and peak E in Figure 4(b)). In contrast, ^{13}C substitution causes a redshift of ν_{25} by 21 cm^{-1} (Table III). The only other combination mode intense enough to have a noticeable effect on the spectrum is $\nu_{13} + \nu_{15} = 2218$ cm^{-1} (I = 0.88 km mol^{-1}), which we expect is responsible for the shoulder at ∼2220 cm^{-1} in the experimental spectrum (peaks C and G in Figures 4(a) and 4(b)).

The weak band D centered at 2140 cm^{-1} in Figure 4(a) is assigned to the fundamental, symmetric stretch of the NCCCO moiety ν_{24} calculated at 2135 cm^{-1} (I = 24.6 km mol^{-1}). Two combination bands $\nu_7 + \nu_{17}$ (2126 cm^{-1}; I = 1.94 km mol^{-1}) and $\nu_{11} + \nu_{15}$ (2136 cm^{-1}; I = 0.48 km mol^{-1}) are too weak to have a significant influence on the spectrum but may be the reason for the broadening of peak D. Note that peak D is redshifted to 2124 cm^{-1} in the ^{15}N isotopomer (peak H, Figure 4(b)) in good agreement with the theoretical prediction (Table III). Peak K at 2080 cm^{-1} in Figure 4(c) may be ascribed to the corresponding absorption in the ^{13}C isotopomer, which is predicted at 2098 cm^{-1} (Table III).

Ph-N=C=C=C=N-Ph 9

Bisiminopropadienes RN=C=C=C=NR′ have been generated from two different types of precursor.[20] These compounds are generally highly unstable and can only be isolated at low temperatures. The diphenyl derivative **9** was obtained by FVT of the isoxazolone precursor **8** (Scheme 4) at 800 °C

TABLE III. Anharmonic wavenumbers ν (cm^{-1}), principal assignments, and dominant contribution (%) for Ph-NCCCO **1b** and its isotopomers in the range 2100–2315 cm^{-1} (see Table S1 for the full set of data).

	Ph-NCCCO **1b**				Ph-^{15}NCCCO		Ph-NCC^{13}CO	
		%	ν (cm^{-1})		ν (cm^{-1})		ν (cm^{-1})	
Mode	Description		ν_{exp}	ν_{theor}	ν_{exp}	ν_{theor}	ν_{exp}	ν_{theor}
$\nu_7+\nu_{17}$	$\alpha_{CCC} + \nu_{CC\ cycle} + (\nu_{CN})$	88		2126		2120		2118
ν_{24}	$\nu_{CC\ sym,\ NCCCN}$	93	2140	2135	2124	2119	∼2080	2098
$\nu_{11}+\nu_{15}$	$\alpha_{CCC\ Cycle} + \delta_{CH\ cycle}$	90	2143	2136		2137	2123	2138
$\nu_{12}+\nu_{15}$	$\delta_{CH\ Cycle}$	94		2160		2159	2147	2160
$\nu_{12}+\nu_{16}$	$\delta_{CH\ Cycle} + \nu_{CCC} + \nu_{CN}$	86						2191
$\nu_{13}+\nu_{15}$	$\delta_{CH\ Cycle}$	82	∼2220	2218	∼2220	2216	…	
ν_{25}	$\nu_{CC\ asym,\ NCCCN}$	71	2243	2254[a]	2242	2251	2222	2224
$\nu_{12}+\nu_{17}$	$\delta_{CH\ Cycle} + \nu_{CC\ cycle}$	66	2247	2264[a]	2245	2265		2264
$\nu_{12}+\nu_{18}$	$\delta_{CH\ Cycle} + \nu_{CC\ cycle}$	79		2312		2312		2312

[a]I > 500 km mol^{-1}.

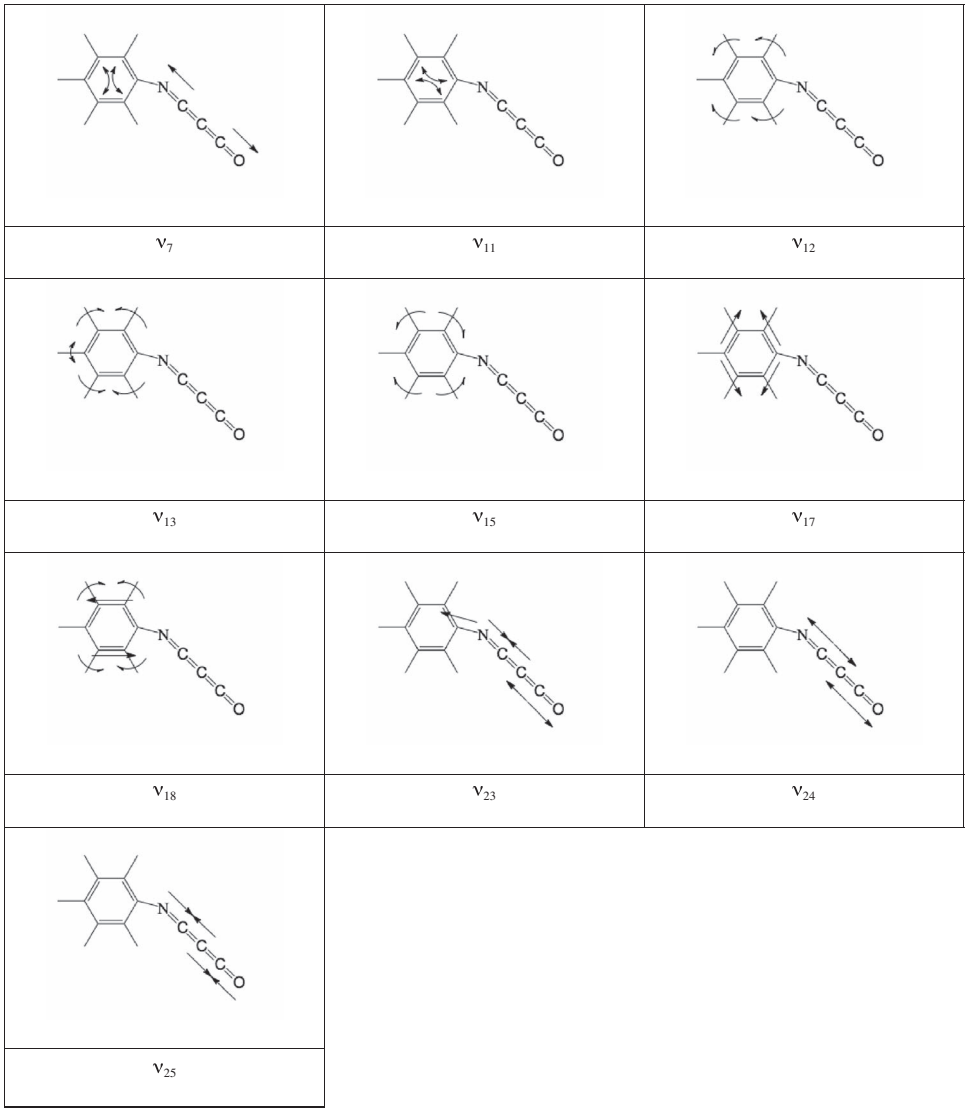

FIG. 5. Description of the modes involved in active fundamental overtones and combination bands in the 2100–2300 cm^{-1} region for **1b**.

and isolated in Ar matrix at 12 K (Figure S4 in the supplementary material[21]). Here, a splitting of the very strong cumulene absorption near 2170 cm^{-1} into three principal components is observed (Figure 6 and Table IV). The fundamental vibrational modes are depicted in Figure 7.

The distinctive peak in the cumulene region of **9** corresponds to the antisymmetric NCCCN stretching ν_{46} = 2168 cm^{-1} (I > 500 km mol^{-1}) giving rise to a strong triplet at 2156–2175 cm^{-1} labeled ABC in Figure 6. The corresponding signature of its isopotomer Ph-^{15}NCCCN-Ph shows a single strong band at 2166 cm^{-1} (peak F) together with a shoulder near 2136 cm^{-1} (peak G, Figure 6). In contrast, the isopotomer Ph-N^{13}CCCN-Ph again shows a single intense band redshifted to 2140 cm^{-1} (peak J, Figure 6). Clearly, the fundamental mode ν_{46} is the most intense, and frequency shifts due to the isotopic labelings are well described by the calculations (Table IV).

Moreover, the calculations predict a strong mode ν_{44} ($\nu_{as,CCCN}$ + $\nu_{CC,cycle}$) near 1580 cm^{-1} (I = 171 km mol^{-1}) and observed experimentally at 1584 cm^{-1} for **9** (Figure S4 and Table S2 in the supplementary material[21]) and corresponding strong bands for the isopotomers Ph-^{15}NCCCN-Ph (1567 cm^{-1}, I = 249 km mol^{-1}) and Ph-N^{13}CCCN-Ph (1578 cm^{-1}, I = 605 km mol^{-1}). This mode gives all or a part of its intensity to the modes 3 and 4 through the combinations ν_3 + ν_{44} (I = 8.60 km mol^{-1}) and ν_4 + ν_{44} (I > 500 km mol^{-1}), thereby resulting in two strong bands located near the fundamental ν_{46} (2180 and 2183 cm^{-1}; see Table IV). Thus, these intense modes explain the appearance of the complex triplet band labeled ABC in Figure 6(a). Isotopic labeling has a significant impact on the frequency

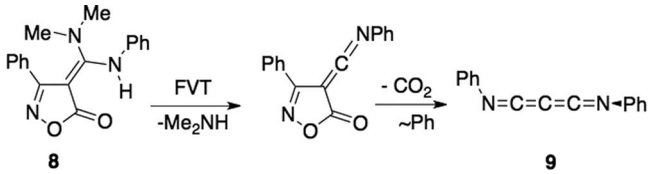

SCHEME 4. Generation of bis(phenylimino)propadiene, Ph-N=C=C=C=N-Ph **9**.

TABLE IV. Anharmonic wavenumbers ν (cm^{-1}), principal assignments, and dominant contribution (%) for Ph-NCCCN-Ph **9** and its isotopomers in the range 2000–2250 cm^{-1} (see Table S2 for the full set of data).

		Ph-NCCCN-Ph **9**			Ph-^{15}NCCCN-Ph		Ph-N^{13}CCCN-Ph	
		%	ν (cm^{-1})		ν (cm^{-1})		ν (cm^{-1})	
Mode	Description		ν_{exp}	ν_{theor}	ν_{exp}	ν_{theor}	ν_{exp}	ν_{theor}
ν_{45}	$\nu_{CC\text{-}NC\ sym,\ NCCCN}$	95	2060	2030	2055	2020	...	1996
$\nu_{24}+\nu_{25}$	$\delta_{CH\ Cycle}$	97		2105				
$\nu_{7}+\nu_{39}$	$\alpha_{NCCCN} + \nu_{CC\ cycle}$	91		2116		2116		2115
$\nu_{23}+\nu_{26}$	$\delta_{CH\ Cycle} + \nu_{CN}$	92					2118	2127
$\nu_{15}+\nu_{32}$	$\alpha_{CCC} + \nu_{NCCCN} + \nu_{CC\ cycle}$	83	2138	2143	2136	2142	...	2145
ν_{46}	$\nu_{CC\text{-}NC\ asym,\ NCCCN}$	79	2156	2168[a]	2166	2160	2140	2152
$\nu_{3}+\nu_{44}$	$\alpha_{CCC} + \nu_{NCCCN} + \nu_{CC\ cycle}$	88	2162	2180		2164	2165	2171
$\nu_{4}+\nu_{44}$	$\alpha_{CCC} + \nu_{NCCCN} + \nu_{CC\ cycle}$	66	2175	2183[a]		2170		2176
$\nu_{24}+\nu_{28}$	$\delta_{CH\ Cycle}$	91						2189
$\nu_{7}+\nu_{41}$	$\alpha_{NCCCN} + \nu_{CC\ cycle}$	94		2204				2197

[a]I > 500 km/mol.

position of the vibrator 44, which leads to reduced couplings between modes 44, 3, and 4 for the two isopotomers, thus resulting in the much sharper peaks F and J in Figure 6(b) and 6(c). The diminution of the activity of these combination modes ($\nu_3 + \nu_{44}$ and $\nu_4 + \nu_{44}$), especially for Ph-^{15}NCCCN-Ph, allows other, weaker combination modes to be observed. Thus the weak combinations described as $\nu_{14} + \nu_{32}$ (2138 cm^{-1}; I = 0.32 km mol^{-1}), $\nu_{15} + \nu_{32}$ (2145 cm^{-1}; I = 3.70 km mol^{-1}), and $\nu_{22} + \nu_{27}$ (2130 cm^{-1}; I = 0.97 km mol^{-1}) may be responsible for peak G in the spectrum of Ph-^{15}NCCCN-Ph (Figure 6(b)).

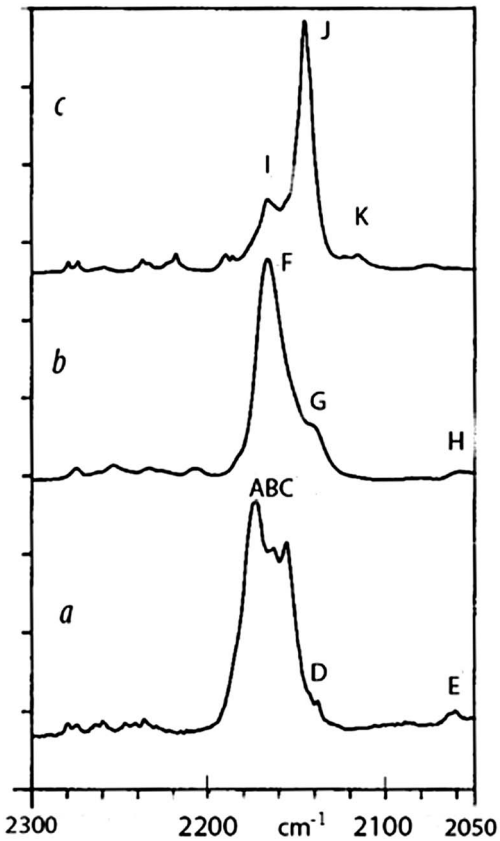

FIG. 6. IR spectra (Ar matrix, 12 K) of PhN=C=C=C=NPh **9** and its isotopomers as generated by FVT of **8** at 800 °C: (a) unlabeled, (b) Ph^{15}NCCCNPh, and (c) PhN^{13}CCCNPh. Peaks A: 2175; B: 2162; C: 2156; D: 2138; E: 2060; F: 2166; G: 2136; H: 2055; I: 2165; J: 2140; K: 2118 cm^{-1}.

As seen in Figure 6, for both systems Ph-NCCCN-Ph and Ph-^{15}NCCCN-Ph, a weak signal corresponding to the symmetrical stretching vibrator NCCCN is observed in the 2050–2000 cm^{-1} region (ν_{45}; bands E and H). For the Ph-N^{13}CCCN-Ph isotopomer, the signal is expected to be red-shifted due to the mass effect, but the band became too weak to be observed.

CONCLUSION

The complex absorption pattern observed in the 2100–2300 cm^{-1} region for methyliminopropadienone, MeN=C=C=C=O **1a** (Figure 1) is singular: **1a** was obtained from four different precursors and the same splitting in this spectral area is observed. The splitting remained after repeated annealing. This makes site splitting highly unlikely. Moreover, in the cases of **1b** and **9** too, annealing did not remove the splitting, and site effects would not explain why different patterns are observed for the isotopomers.

Finally, we showed that the complex absorption pattern observed in the 2100–2300 cm^{-1} region for methyliminopropadienone, MeN=C=C=C=O **1a** (Figure 1) is ascribed to the presence of the overtone $2\nu_6$ and the combination band $\nu_5 + \nu_6$ near the fundamental NCCCO antisymmetric stretch, ν_{12}. Furthermore, the combination $\nu_4 + \nu_6$ gives rise to a splitting of the fundamental NCCCO symmetric stretch ν_{11} at 2163 and 2126 cm^{-1}. The mode ν_6 is associated with deformation of the CH_3 group, and thus will not be observed for differently substituted iminopropadienones.

In PhN=C=C=C=O **1b** the antisymmetric stretch of the NCCCO moiety is split into two strong bands at 2247 and 2243 cm^{-1} (Figure 4) ascribed to the combination mode $\nu_{12} + \nu_{17}$ and the fundamental ν_{25}, respectively.

In PhN=C=C=C=NPh **9** the mode ν_{44} ($\nu_{as,CCCN} + \nu_{CC,cycle}$) gives rise to two strong combination modes $\nu_3 + \nu_{44}$ and $\nu_4 + \nu_{44}$ located near the antisymmetric NCCCN stretch ν_{46}, thereby giving rise to the tripling of the major band in the region 2156–2175 cm^{-1} (Figure 6).

This work demonstrates that calculations of anharmonic vibrational modes are invaluable for the correct characterization of reactive intermediates and unusual molecules by matrix-isolation infrared spectroscopy. The major spectral features could not have been interpreted on the basis of harmonic vibrational calculations alone. In general, the analysis of the additional information inherent in combination bands and overtones makes for more secure characterization.

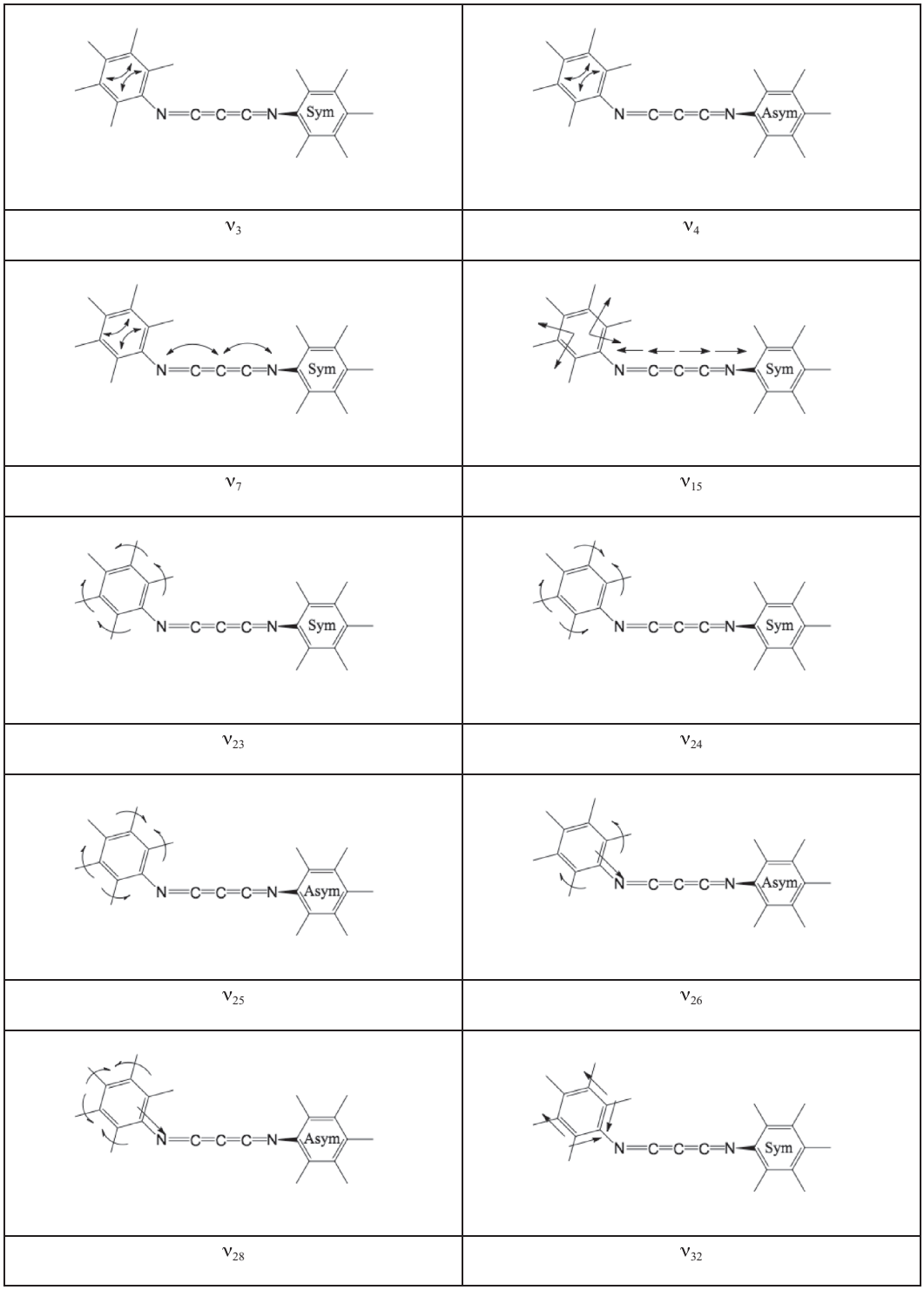

FIG. 7. Description of the modes implicated in active fundamental, overtones, and combination bands in the 2000–2200 cm^{-1} region for **9**.

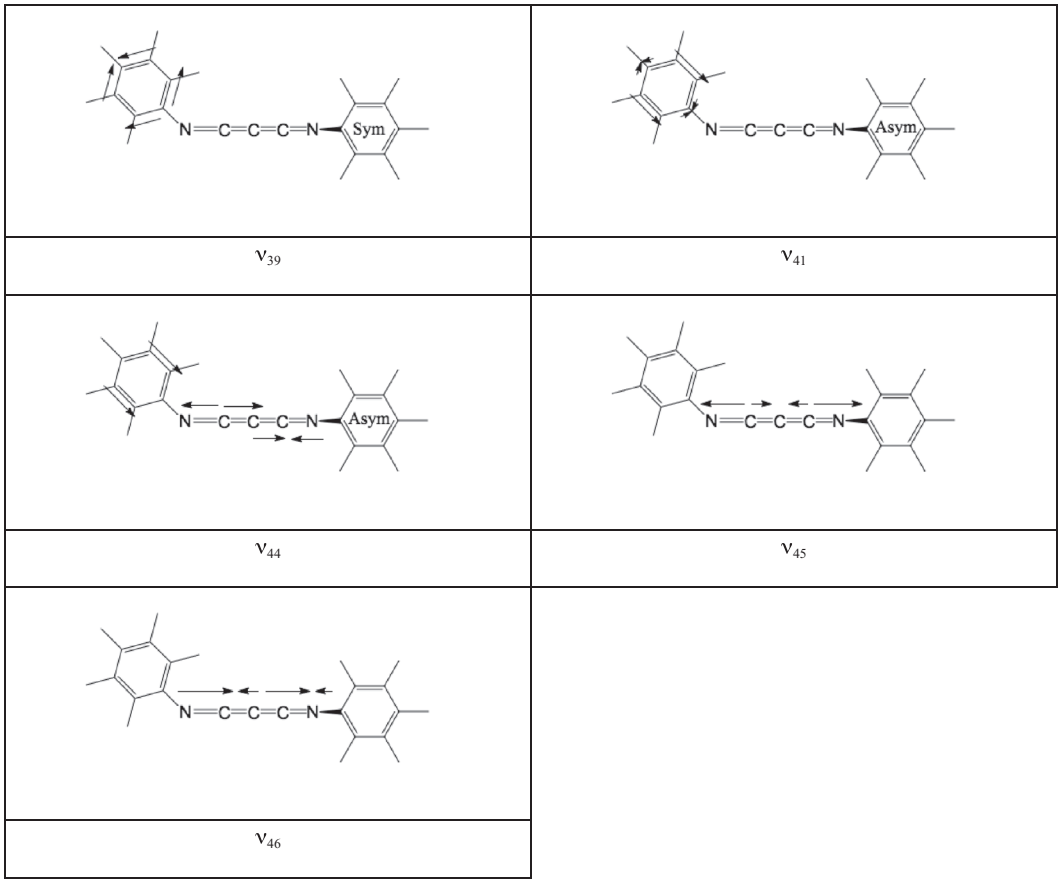

FIG. 7. (*Continued.*)

ACKNOWLEDGMENTS

The Australian Research Council and The University of Queensland supported this work. Computer time for this study was provided by the computing facilities MCIA (Mésocentre de Calcul Intensif Aquitain) of the Université de Bordeaux and of the Université de Pau et des Pays de l'Adour. The authors declare no competing financial interest.

[1]I. R. Dunkin, *Matrix-Isolation Techniques* (Oxford University Press, Oxford, UK, 1998); T. Bally, in *Reactive Intermediate Chemistry*, edited by R. A. Moss, M. S. Platz and M. Jones, Jr. (Wiley, Hoboken, NJ, 2004).
[2]D. Bégué, N. Gohaud, C. Pouchan, P. Cassam-Chenai, and J. Lievin, J. Chem. Phys. **127**, 164115 (2007).
[3]D. Bégué, P. Labeguerie, D. Y. Zhang-Negrerie, A. Avramopoulos, L. Serrano-Andres, and M. G. Papadopoulos, Phys. Chem. Chem. Phys. **12**, 13746–13751 (2010).
[4]D. Bégué, I. Baraille, P.-A. Garrain, A. Dargelos, and T. Tassaing, J. Chem. Phys. **133**, 034102 (2010); I. Baraille, C. Larrieu, A. Dargelos, and M. Chaillet, Chem. Phys. **273**, 91 (2001).
[5]D. Bégué, G. G. Qiao, and C. J. Wentrup, Am. Chem. Soc. **134**, 5339 (2012).
[6]T. Mosandl, C. O. Kappe, R. Flammang, and C. Wentrup, J. Chem. Soc., Chem. Commun. **21**, 1571–1573 (1992); C. Wentrup, V. V. Ramana Rao, W. Frank, B. E. Fulloon, D. W. J. Moloney, and T. Mosandl, J. Org. Chem. **64**, 3608–3619 (1999); D. Lecoq, B. A. Chalmers, R. N. Veedu, D. Kvaskoff, P. V. Bernhardt, and C. Wentrup, Aust. J. Chem. **62**, 1631–1638 (2009).
[7]T. Mosandl, S. Stadtmüller, M. W. Wong, and C. Wentrup, J. Phys. Chem. **98**, 1080–1086 (1994).
[8]D. W. J. Moloney, M. W. Wong, R. Flammang, and C. Wentrup, J. Org. Chem. **62**, 4240–4247 (1997).
[9]R. Flammang, Y. Van Haverbeke, M. W. Wong, A. Rühmann, and C. Wentrup, J. Phys. Chem. **98**, 4814–4820 (1994).
[10]A. Chrostowska, A. Dargelos, S. Khayar, and C. Wentrup, J. Phys. Chem. A **116**, 9315–9320 (2012).
[11]C. Lee, W. Yang, and R. G. Parr, Phys. Rev. B **37**, 785 (1988); A. D. Becke, J. Chem. Phys. **98**(2), 1372–1377 (1993).
[12]M. J. Frisch, G. W. Trucks, H. B. Schlegel *et al.*, Gaussian 09, Revision B.2, Gaussian, Inc., Wallingford, CT, 2009.
[13]C. O. Kappe, Ph.D. thesis, The University of Queensland, Australia and Universität Graz, Austria, 1992; D. W. J. Moloney, Ph.D. thesis, The University of Queenaland, Australia, 1997.
[14]H. G. Andersen and C. Wentrup, Aust. J. Chem. **65**, 105–112 (2012).
[15]C. Plüg, W. Frank, and C. Wentrup, J. Chem. Soc., Perkin Trans. 2 **6**, 1087 (1999); H. G. Andersen, U. Mitschke, and C. Wentrup, *ibid.* **4**, 602 (2001).
[16]H.-J. Werner, P. J. Knowles, G. Knizia, F. R. Manby, M. Schütz *et al.*, MOLPRO, version 2012.1, a package of *ab initio* programs, 2012, see http://www.molpro.net.
[17]P. Jensen and J. W. C. Johns, J. Mol. Spectrosc. **118**, 248 (1986); J. Koput, Chem. Phys. Lett. **320**, 237 (2000).
[18]N. Gohaud, D. Bégué, and C. Pouchan, Int. J. Quantum Chem. **104**, 773–781 (2005).
[19]D. Bégué, S. Elissalde, E. Pere, P. Iratcabal, and C. Pouchan, J. Phys. Chem. A **110**, 7793–7800 (2006).
[20]R. Wolf, S. Stadtmüller, M. W. Wong, M. Barbieux-Flammang, R. Flammang, and C. Wentrup, Chem.-Eur. J. **2**, 1318–1329 (1996); H. G. Andersen, D. Kvaskoff, and C. Wentrup, Aust. J. Chem. **65**, 686–689 (2012).
[21]See supplementary material at http://dx.doi.org/10.1063/1.4826647 for additional Ar matrix IR spectra of **1a** generated from **4a** (650 °C) and **5** (800 °C), of **1b** generated from **2b** at 600 °C, and of **9** generated from **8** at 800 °C (Figures S1–S4). Experimental section with procedures for the generation and matrix isolation of **1a**, **1b,** and **9**. Cartesian coordinates and energies of calculated structures, and details of calculated anharmonic wavenumbers and spectroscopic descriptions.